Simultaneous Optimization of Renewable Energy and Energy Storage Capacity with the Hierarchical Control

Zhaodi Shi, Weisheng Wang, *Member, IEEE*, Yuehui Huang, Pai Li, and Ling Dong

***Abstract*—To fully consider the complementary role of different energy sources and reduce the curtailment of renewable energy (RE) in high RE penetration systems, a hierarchical optimization algorithm is proposed to simultaneously optimize the capacity of RE generation and energy storage systems (ESS). Time sequence simulation (TSS) technology is adopted to fully consider the regional RE resource characteristics and make the model more reliable. An optimization model for evaluating ESS capacity is established at a lower level. To overcome the high dimensional complexity of time sequence data, this paper re-formulates this sub-model as a consensus problem, which can be solved by a distributed approach to minimize the system's total investment costs. At the upper level, the model for assessing the proportion of wind and solar capacity is developed by maximizing the RE generation. The golden section Fibonacci tree optimization (GSFTO) algorithm is utilized to improve the efficiency and solution accuracy. The results show that the algorithm and model are feasible and applicable for the identified purposes, which can provide a useful guidance for the development of power generation and the energy storage capacity in high RE penetration systems.**

***Index Terms*—Consensus problem, energy storage, planning, renewable, time sequence simulation (TSS).**

NOMENCLATURE

S	Set of ESS types.
s	ESS types.
$\eta_{\mathrm{c}}^{\mathrm{s}}, \eta_{\mathrm{d}}^{\mathrm{s}}$	Charged/discharged energy efficiency.
$\zeta_{\mathrm{es}}^{\mathrm{s}}$	Self-discharging rate.
a^{s}	Amortization factor.
$E_{\mathrm{t}}^{\mathrm{s}}$	Energy in ESS s at time t.
$P_{\mathrm{t}}^{\mathrm{s},+}, P_{\mathrm{t}}^{\mathrm{s},-}$	Charged/discharged energy at time t.
$E_{\max}^{\mathrm{s}}, E_{\min}^{\mathrm{s}}$	Maximum/minimum ESS capacity.
$\varpi_{\max}^{\mathrm{s}}, \varpi_{\min}^{\mathrm{s}}$	Upper/lower coefficient of ESS s.
$E_{\mathrm{bat}}^{\mathrm{s}}$	Battery capacity of ESS s.
$u_{\mathrm{t}}^{\mathrm{s},+}, u_{\mathrm{t}}^{\mathrm{s},-}$	Charge/discharge state of storage s.
$\delta_{\mathrm{es}}^{\mathrm{s}}$	Rated power/energy ratio.
$C_{\mathrm{t}}^{\mathrm{s}}$	Cost of storage s at time t.
$c_{\mathrm{inv}}^{\mathrm{s}}$	Investment cost of storage s.
c_{w}	Investment cost of wind turbine.
c_{pv}	Investment cost of solar panel.
$P_{\mathrm{t}}^{\mathrm{P}}$	Power output of PV plant.
$P_{\mathrm{t}}^{\mathrm{W}}$	Power output of wind plant.
E_{pv}	Installed capacity of PV plant.
E_{w}	Installed capacity of wind plant.
$p_{\mathrm{t}}^{\mathrm{P}}$	Normalized PV generation.
$p_{\mathrm{t}}^{\mathrm{w}}$	Normalized wind generation.
$P_{\mathrm{t}}^{\mathrm{l}}$	Tie-line power at time t.
η_{RE}	Curtailment ratio of renewable energy.
T	Planning horizon.
I	Set of all sub horizons.
$z_{\mathrm{d}}^{i}, z_{\mathrm{b}}^{i}$	Design/boundary parameters.
$g_{\mathrm{d}}, g_{\mathrm{b}}$	Global design/boundary parameters.
C^{i}	Feasible set of design variables.
$\boldsymbol{v}_0^{i}, \boldsymbol{v}_{\mathrm{T}}^{i}$	Beginning/end storage capacity of horizon.
$\{\boldsymbol{x}^{i}\}$	Dual variables.
τ	Update step size of dual variable.
k	Iteration number.
$\mathbf{B}$	Group index mapping.
B	Element-wide index mapping.
χ	Designed variables in lower level model.
E_{RE}	Installed capacity of RE generation.
F_i	The ith item of the Fibonacci sequence.
R	Set of processing points of FTO.
W	Vector dimension of F_i.
$x_{\mathrm{ub}}, x_{\mathrm{lb}}$	Upper/lower bound of the F_i.
$N_{\max}$	Maximum depth of the Fibonacci tree.
$I_{\mathrm{c},i}$	Indicator to record the constraint conflict situation.

Manuscript received July 4, 2019; revised September 26, 2019; accepted January 7, 2020. Date of online publication February 13, 2020; date of current version May 28, 2020. This work was supported jointly by the National Key R&D Program of China (2017YFB0902200); State Grid Corporation of China Science and Technology Project (5228001700CW) and the Qinghai Province Science and Technology Plan (2018-GX-A6).

Z. D. Shi (corresponding author, e-mail: shizd91@163.com), W. S. Wang, Y. H. Huang and P. Li are with the State Key Laboratory of Operation and Control of Renewable Energy and Storage Systems, China Electric Power Research Institute, Beijing 100192, China.

L. Dong is with the State Grid Qinghai Electric Power Company, Xining 810000, China.

DOI: 10.17775/CSEEJPES.2019.01470

I. INTRODUCTION

THE development of renewable energy (RE) is significant to cope with an energy crisis and environmental pollution [1], [2]. RE sources have remarkable characteristics of variability and uncertainty, and energy storage systems (ESS) can provide flexibility to mitigate the impact of RE access to the grid [3], [4].

The planning standards of RE and ESS capacities in power systems are different from previous standards. In the past, RE capacity in the grid was small and ESS was planned without considering RE characteristics. With large-scale RE sources

connected to the grid, various ESS technologies are studied as a mitigation of RE variability and uncertainty. Simultaneous optimization of RE generation and ESS capacity for the RE-ESS power plant are key issue for the future economic viability of these RE resources [5]. Traditional methods usually plan ESS and RE generation capacity separately, the ESS capacity is normally guided according to the demand [6]–[9], which is easy to be solved by meeting certain specified reliability indices. However, without considering the RE generation feature, the needed flexibility of ESS as a means of ensuring peak cut is small, and the planned ESS capacity also will be reduced. So, the planned ESS capacity usually is too conservative, resulting in an increase in RE curtailment. In addition, this method is not suitable of those power delivery systems without local demand. Thus, in this work, we simultaneously optimize capacity of ESS and RE generation in the high RE penetration system.

In recent years, scholars at home and abroad are paying attention to the topic of capacity planning of ESS and RE. The hybrid ESS and RE generation capacity is optimized in [10] and [11] by some distributed optimization framework. However, they all just optimize the energy storage and RE capacity separately. Some studies have been conducted on isolated grid planning and/or operation of specific types of ESS [11]–[16]. The power constraint of the transmission line is rarely considered, so they are not suitable for interconnected systems.

The power system capacity planning model generally takes the system cost as the objective function. Simultaneously planning the capacity of ESS and RE generation means an increase in decision variables and higher model dimensions, which brings greater challenges to the solution. In addition, the RE curtailment has become a serious problem in some regional systems of China, therefore, another goal in this paper is to relief the RE curtailment. We use a bi-level model to solve multi-objective optimization problems [17], [18] and reduce the difficulty of model solving.

An annual RE long-term time sequence is generally adopted in planning models. The accurate probability density function of RE generation usually is difficult to obtain to reflect the RE complex characteristics. The existing research usually adopts a typical day [19] method or Monte Carlo stochastic simulation method [20], [21]. For example, the authors in [22] statistically analyze the typical weather data to obtain the output of typical PV generation. The authors in [23] proposed a stochastic, multistage, co-planning model of transmission expansion with ESS. To some extent, both methods have been well applied in specific scenarios. However, the typical day method is difficult to reflect annual output characteristics of RE power, while the stochastic simulation method cannot indicate the temporal characteristics of RE power. In addition, another limitation of the existing renewable generation planning problem is the difficulty to obtain various annual RE sequences in the region [24], existing methods generally only use historical data, which reduces the confidence in capacity planning results due to the small sample size. Therefore, time sequence simulation (TSS) technology [25] is used in this paper to obtain the RE sequence. One of the main advantages of TSS is the annual RE planning can be incorporated into the power system, so it is more scientific and reasonable. In addition, based on TSS, this paper can generate multiple time sequences of RE according to historical data to meet the RE characteristics of the region, which can be used to solve the planning model and make the planning results more general.

Based on our previous description and discussion, this paper proposes a hierarchical optimization algorithm to jointly plan the capacity of RE power and ESS. The TSS method is adopted to generate the wind and PV sequences while considering the time characteristics, as well as generating multiple sets of RE output sequences for capacity planning to increase the reliability of planning results. The ESS capacity is optimized in the lower level, the object function is the minimum total investment cost while comprehensively considering constraints, such as storage charge- discharge characteristics, RE curtailment rates and so on. This model is a mixed integer liner programming (MILP) problem and the annual time sequence of RE is adopted as input. However, the planning horizon of the problem increases with the larger size of the data, which causes increasingly difficulties in solving the problem. Therefore, we rewrite the original lower level problem as a consensus problem [26], which can be solved by the alternating direction multiplier method (ADMM) in a parallel distribution manner [27]. The upper level is used to optimize the capacity of the wind and solar plants, and total renewable generation is used as the fitness function to update the optimization direction of the search elements. The golden section Fibonacci tree optimization (GSFTO) algorithm [28] is adopted to solve the problem, which avoids the problem of the algorithm's convergence ability decreasing near the optimal solution and the iteration process taking much more time in the long-term planning models [29], [30]. The simulation cases prove the rationality of the proposed model and the feasibility of the algorithm. It has a guiding significance for the formulation of RE generation and the ESS capacity in high renewable penetration systems.

This paper is organized as follows. We describe the system model in Section II. Section III formulates the optimization problem. The proposed algorithms for solving the planning model are introduced in Section IV. Section V provides examples and results. The last section is the conclusion.

II. System Models

A. Energy Storage Model

ESS is characterized by some parameters, and the following equation is satisfied:

$$E_{t+1}^{\mathrm{s}} = \begin{cases} E_{\mathrm{t}}^{\mathrm{s}} - \dfrac{1}{\eta_{\mathrm{c}}^{\mathrm{s}}} P_{\mathrm{t}}^{\mathrm{s}} \Delta t - \zeta_{\mathrm{es}}^{\mathrm{s}} E_{\mathrm{t}}^{\mathrm{s}} & \text{if } P_{\mathrm{t}}^{\mathrm{s}} \geq 0 \\ E_{\mathrm{t}}^{\mathrm{s}} - \eta_{\mathrm{d}}^{\mathrm{s}} P_{\mathrm{t}}^{\mathrm{s}} \Delta t - \zeta_{\mathrm{es}}^{\mathrm{s}} E_{\mathrm{t}}^{\mathrm{s}} & \text{if } P_{\mathrm{t}}^{\mathrm{s}} < 0 \end{cases} \tag{1}$$

where $P_{\mathrm{t}}^{\mathrm{s}} \geq 0$ denotes ESS discharging power, $P_{\mathrm{t}}^{\mathrm{s}} \leq 0$ denotes ESS charging power. Then we have the following substitution:

$$P_{\mathrm{t}}^{\mathrm{s}} = P_{\mathrm{t}}^{\mathrm{s},+} - P_{\mathrm{t}}^{\mathrm{s},-}, P_{\mathrm{t}}^{\mathrm{s},+} \geq 0, P_{\mathrm{t}}^{\mathrm{s},-} \geq 0 \tag{2}$$

So we rewrite (1) as:

$$E_{t+1}^{\mathrm{s}} = E_{\mathrm{t}}^{\mathrm{s}} + \eta_{\mathrm{d}}^{\mathrm{s}} P_{\mathrm{t}}^{\mathrm{s},-} \Delta t - \frac{1}{\eta_{\mathrm{c}}^{\mathrm{s}}} P_{\mathrm{t}}^{\mathrm{s},+} \Delta t - \zeta_{\mathrm{es}}^{\mathrm{s}} E_{\mathrm{t}}^{\mathrm{s}} \tag{3}$$

The state of charge (SOC) constraint is composed of (3) and the following equations.

$$E^{\mathrm{s}}_{\min} \le E^{\mathrm{s}}_{\mathrm{t}} \le E^{\mathrm{s}}_{\max} \tag{4}$$

$$E^{\mathrm{s}}_{\max} = \varpi^{\mathrm{s}}_{\max} E^{\mathrm{s}}_{\mathrm{bat}} \tag{5}$$

$$E^{\mathrm{s}}_{\min} = \varpi^{\mathrm{s}}_{\min} E^{\mathrm{s}}_{\mathrm{bat}} \tag{6}$$

The minimum and maximum SOC of ESS are assumed to be 20% and 95% of the installed energy capacity [31].

ESS needs to satisfy the continuity constraint as follows:

$$E^{\mathrm{s}}_{t+1} = E^{\mathrm{s}}_{\mathrm{t}} + \frac{\eta^{\mathrm{s}}_{\mathrm{c}} P^{\mathrm{s},+}_{t+1}}{E^{\mathrm{s}}_{\mathrm{bat}}}\Delta t - \frac{P^{\mathrm{s},-}_{t+1}}{\eta^{\mathrm{s}}_{\mathrm{d}} E^{\mathrm{s}}_{\mathrm{bat}}}\Delta t \tag{7}$$

Additionally, the charging/discharging state constraints are shown as follows:

$$\begin{cases} 0 \le u^{\mathrm{s},+}_{\mathrm{t}} + u^{\mathrm{s},-}_{\mathrm{t}} \le 1 \\ u^{\mathrm{s},+}_{\mathrm{t}}, u^{\mathrm{s},-}_{\mathrm{t}} \in \{0,1\} \end{cases} \tag{8}$$

where $u^{\mathrm{s},+}_{\mathrm{t}}$ and $u^{\mathrm{s},-}_{\mathrm{t}}$ are 0–1 integer variables, $u^{\mathrm{s},+}_{\mathrm{t}} = 1$ denotes the storage is charging and $u^{\mathrm{s},+}_{\mathrm{t}} = 0$ denotes the storage is not charging; Meanwhile $u^{\mathrm{s},-}_{\mathrm{t}}$ indicates the discharge state of storage s.

$$0 \le P^{\mathrm{s},+}_{\mathrm{t}} \le u^{\mathrm{s},+}_{\mathrm{t}} P^{\mathrm{s},+}_{\max} \tag{9}$$

$$0 \le P^{\mathrm{s},-}_{\mathrm{t}} \le u^{\mathrm{s},-}_{\mathrm{t}} P^{\mathrm{s},-}_{\max} \tag{10}$$

$$P^{\mathrm{s},+}_{\max} = \eta^{\mathrm{s}}_{\mathrm{c}} \delta^{\mathrm{s}}_{\mathrm{es}} E^{\mathrm{s}}_{\max} \tag{11}$$

$$P^{\mathrm{s},-}_{\max} = (1/\eta^{\mathrm{s}}_{\mathrm{d}}) \delta^{\mathrm{s}}_{\mathrm{es}} E^{\mathrm{s}}_{\max} \tag{12}$$

If $\delta^{\mathrm{s}}_{\mathrm{es}}$ is not fixed, another designed variable can be introduced. The investment cost is modified and defined by both $E^{\mathrm{s}}_{\max}$ and $\{P^{\mathrm{s},+}_{\max}, P^{\mathrm{s},-}_{\max}\}$.

$$C^{\mathrm{s}}_{\mathrm{t}} = a^{\mathrm{s}} c^{\mathrm{s}}_{\mathrm{inv}} E^{\mathrm{s}}_{\max} \tag{13}$$

Due to substitution (2), the constraints (1) and (3) are equivalent if only one element of each pair $\{P^{\mathrm{s},+}_{\max}, P^{\mathrm{s},-}_{\max}\}$ is non-zero for all s, t [32].

B. Generator Model

All generators in this model are renewable generators, the power stations include wind farms and the PV station.

1) PV Power Generation Constraint

$$0 \le P^{\mathrm{p}}_{\mathrm{t}} \le p^{\mathrm{p}}_{\mathrm{t}} E_{\mathrm{pv}} \tag{14}$$

2) Wind Power Generation Constraint

$$0 \le P^{\mathrm{w}}_{\mathrm{t}} \le p^{\mathrm{w}}_{\mathrm{t}} E_{\mathrm{w}} \tag{15}$$

C. Tie Line Power Constraint

$$P^{\mathrm{w}}_{\mathrm{t}} + P^{\mathrm{p}}_{\mathrm{t}} + \sum_{s\in S}(P^{\mathrm{s},-}_{\mathrm{t}} - P^{\mathrm{s},+}_{\mathrm{t}}) \le P^{\mathrm{l}}_{\mathrm{t}}, \forall t \tag{16}$$

D. RE Curtailment Constraint

In addition to reducing the RE curtailment, we consider the curtailment rate constraint:

$$(1-\eta_{\mathrm{RE}}) \sum_{t\in T}(E_{\mathrm{w}} p^{\mathrm{w}}_{\mathrm{t}} + E_{\mathrm{pv}} p^{\mathrm{p}}_{\mathrm{t}}) \le \sum_{t\in T}(P^{\mathrm{w}}_{\mathrm{t}} + P^{\mathrm{p}}_{\mathrm{t}}) \tag{17}$$

III. RE Generation and ESS Capacity Planning

A. Optimal Planning Problem in the Lower Level

For RE units such as wind and solar power plants and energy storage batteries considered in this paper, their operation and maintenance costs usually account for less than 10% of the investment cost of capacity, therefore, it has less impact on capacity planning results. The existing methods usually combine the capacity investment cost and the operational and maintenance costs, and then simplify the model for easy solution. Practice has shown that this method can be used in capacity planning of high RE penetration systems. Therefore, in this paper, we ignore the power cost of ESS.

The wind/solar/ESS model is established to optimize storage capacity in the lower level. The planning objective in the lower level model is to find the optimal capacity of ESS by minimizing the total investment cost, allowing for most of the needs of the power grid to be satisfied. The objective function is the minimum investment cost of the energy storage battery and RE power plants in the system:

$$f(E_{\max}, \chi_{\max}) = \sum_{t\in T}(\sum_{s\in S}(a^{\mathrm{s}} c^{\mathrm{s}}_{\mathrm{inv}} E^{\mathrm{s}}_{\max}) + (c_{\mathrm{w}} E_{\mathrm{w}} + c_{\mathrm{pv}} E_{\mathrm{pv}})) \tag{18}$$

where $E_{\max}$ denotes the maximum ESS capacity.

Then the optimization problem for ESS capacity planning can be formulated as:

$$\begin{aligned} &\min \ f(E_{\max}, \chi_{\max}) \\ &\text{subject to (1)–(17)} \end{aligned} \tag{19}$$

By the analysis above, the ESS capacity planning model in the high RE penetration system is established in the lower level.

B. Optimal Planning Problem in the Upper Level

The intelligent optimization algorithm is adopted to optimize the installed capacity of wind and solar power in the upper level. It is necessary to give the objective function and variable space constraints to guide the optimization direction of the search element.

1) Objective Function

$$G = \max \sum_{t\in T}(P^{\mathrm{w}}_{\mathrm{t}} + P^{\mathrm{p}}_{\mathrm{t}} + \sum_{s\in S}(P^{\mathrm{s},-}_{\mathrm{t}} - P^{\mathrm{s},+}_{\mathrm{t}})) \tag{20}$$

where G is the objective function to maximize the RE generation, the optimization direction of the search elements in the upper level is updated according to the value of G.

2) Variable Space Constraints

$$0 \le P^{\mathrm{p}}_{\mathrm{t}} \le p^{\mathrm{p}}_{\mathrm{t}} E_{\mathrm{pv}} \tag{21}$$

$$0 \le P^{\mathrm{w}}_{\mathrm{t}} \le p^{\mathrm{w}}_{\mathrm{t}} E_{\mathrm{w}} \tag{22}$$

$$E_{\mathrm{w}} + E_{\mathrm{pv}} = E_{\mathrm{RE}} \tag{23}$$

The objective function and constraints above constitute the model for capacity optimization of wind and PV power based on maximizing power generation. The GSFTO algorithm is used to solve this upper level model.

To sum up, a simultaneous optimization model for optimizing RE generation and ESS capacity is proposed. In actual practice, the relevant constraints can be selected according to the real power grid applications.

IV. Algorithms for Solving the Problem

A. Formulation of the Consensus Problem in the Lower Level

The consensus problem means that the control units in the system are not directly controlled by the centralized control system, but by the distributed control and update their respective states according to their own and neighboring unit information, thereby consistently completing the control objectives. For the purposes of this paper, the wind farms and PV power plants in the lower level model can be coordinated locally by only interacting with the power and capacity information of the adjacent units, so that the external power of the whole RE generation system can meet the needs of the upper level model. In addition, due to the volatility of renewable energy output, historical data is often used to solve planning problems in production time. Due to the randomness of RE, historical data is mostly utilized in the problem formulation, which leads to increasingly difficulties in solving the problem. In this section, the original problem (19) is re-expressed as a consensus problem, which can be solved in a distributed manner.

In this paper, the whole planning horizon T is divided into T^i, then we can get $T = \cup_{i\in I} T^i$. For simplicity, assume T^i is chronologically arranged. $g_{\mathrm{d}} = E_{\max}$ denotes the global design parameters; $z_{\mathrm{d}}^j = E_{\max}^i$ represents the design parameters of the jth scenario; C^i denotes the feasible set for the design variables, $C = \cap_{i\in I} C^i$. An additional assumption is made in [32] that $E_0^i = E_{\mathrm{T}}^i,\ i \in I$, which makes the resulting solution suboptimal. Thus, we abandon this assumption and add the additional consensus constraints to the scenario.

Setting $z_{\mathrm{b}}^j = [E_0^i, E_{\max}^i]$, $g_{\mathrm{b},B(i)}$ as the globing boundary parameters corresponding to $[E_{\mathrm{T}}^{i-1}; E_0^{i+1}]$ and $(z_{\mathrm{b}}^i)_j$ corresponds to $g_{\mathrm{b},B(i,j)}$. Then the constraints $E_0^i = E_{\mathrm{T}}^{i-1}, i \in I$ can be rewritten as $z_{\mathrm{b}}^j = g_{\mathrm{b},B(i)}, i \in I$. Let $z^i = [z_{\mathrm{d}}^i; z_{\mathrm{b}}^i]$, $g = [g_{\mathrm{d}}; g_{\mathrm{b}}]$ and $g_{\mathrm{B}}^i = [g_{\mathrm{d}}; g_{\mathrm{b},B(i)}]$, (19) can be formulated as:

$$\begin{aligned} &\min_{z_{\mathrm{d}}^i \in c^i, z_{\mathrm{b}}^i} \sum_{i\in I} f^i(z^i) \\ &\text{subject to } z^i = g_{\mathrm{B}}^i,\ i \in I. \end{aligned} \tag{24}$$

Solving the problem (24), g_{d} satisfy $g_{\mathrm{d}} \in C$. It is worth noting that, similar to equation (19), we have omitted some optimization variables for non-decision variables for the sake of simplicity in the calculation.

B. Distributed Optimization of Consensus Problem

Due to the number of computational scenarios and time complexity increases, the planning problem becomes more challenging to be solved. In this paper, based on the alternating direction multiplier (ADMM) [33], a distributed manner is proposed to solve (24), which can alleviate the time complexity matter and enhance the extensibility of the model.

In order to perform the consensus (equality) constraint in (24), we introduce a new quadratic term to the problem, and the augmented Lagrangian is shown as follows.

$$\begin{aligned} &L_\tau\left(\left\{z^i\right\}, g, \left\{\boldsymbol{x}^i\right\}\right) = \\ &\quad \sum_{i\in I}\left(f^i\left(z^i\right) + \boldsymbol{x}^{i\mathrm{T}}\left(z^i - g_{\mathrm{B}}^i\right) + \frac{\tau}{2}\left\|z^i - g_{\mathrm{B}}^i\right\|_2^2\right) \end{aligned} \tag{25}$$

Note that the difference between $\{z^i\}$ and g_{B}^i is penalized by the quadratic term.

With the advantages of the simple form, good convergence and strong robustness, ADMM is an algorithm suitable for solving a separable convex optimization. It gradually approaches the optimal solution in parallel by the following iterative steps.

$$\begin{aligned} z_{\mathrm{k}+1}^i &= \arg\min_{\boldsymbol{v}^i} L_\tau\left(\left\{z^i\right\}, g_{\mathrm{k}}, \left\{\boldsymbol{x}^i\right\}\right) \\ &= \arg\min_{z_{\mathrm{d}}^i \in C^i, z_{\mathrm{b}}} f\left(z^i\right) + \boldsymbol{x}^{i\mathrm{T}}\left(z^i - g_{B,k}^i\right) + \frac{\tau}{2}\left\|z^i - g_{B,k}^i\right\|_2^2 \end{aligned} \tag{26}$$

$$\begin{aligned} g_{\mathrm{k}+1} &= \arg\min_{\mathrm{g}} L_\tau\left(\left\{z_{\mathrm{k}+1}^i\right\}, g, \left\{\boldsymbol{x}^i\right\}\right) \\ &= \arg\min_{\mathrm{g}} \sum_{i\in I}\left(\boldsymbol{x}^{i\mathrm{T}}\left(z_{\mathrm{k}+1}^i - g_{\mathrm{B}}^i\right) + \frac{\tau}{2}\left\|z_{\mathrm{k}+1}^i - g_{\mathrm{B}}^i\right\|_2^2\right) \end{aligned} \tag{27}$$

We consider constraints in the consensus problem. So, $g = [g_{\mathrm{d}}; g_{\mathrm{b}}]$ and $g_{\mathrm{B}}^i = [g_{\mathrm{d}}; g_{\mathrm{b},B(i)}]$, which makes (27) difficult to solve, We need to consider g_{d} and g_{b} separately to solve (27), setting $\boldsymbol{x}^i = [\boldsymbol{x}_{\mathrm{d}}^i; \boldsymbol{x}_{\mathrm{b}}^i]$, (27) can be written as follows:

$$\begin{aligned} g_{\mathrm{k}+1} = \arg\min_{\mathrm{g}} \sum_{i\in I}\Bigg(&\boldsymbol{x}_{d,k}^{i\mathrm{T}}\left(z_{d,k+1}^i - g_{\mathrm{d}}\right) + \frac{\tau}{2}\left\|z_{d,k+1}^i - g_{\mathrm{d}}\right\|_2^2 \\ &+ \boldsymbol{x}_{\mathrm{b},k}^{i\mathrm{T}}(z_{\mathrm{b},k+1}^i - g_{\mathrm{b},B(i)}) + \frac{\tau}{2}\left\|z_{\mathrm{b},k+1}^i - g_{\mathrm{b},B(i)}\right\|_2^2\Bigg) \end{aligned} \tag{28}$$

Solving for (28), the results are:

$$g_{d,k+1} = \frac{1}{I}\sum_{i\in I}\left(z_{\mathrm{k}+1}^i + \frac{1}{\tau}\boldsymbol{x}_{d,k}^i\right) \tag{29}$$

$$(g_{\mathrm{b},k+1})_{\mathrm{n}} = \frac{\sum_{B(i,j)\in n}\left((z_{\mathrm{b},k+1}^i)_j + \frac{1}{\tau}(x_{\mathrm{b},k}^i)_j\right)}{\sum_{B(i,j)\in n} 1} \tag{30}$$

The global design variable g_{d} will satisfy each sub-problem constraint when ADMM converges, and $g_{\mathrm{d}} \in C^i, \forall i \in I$, so $g_{\mathrm{d}} \in C$ is obtained.

The update of dual variables $\boldsymbol{x}^i$ is guided by (31) in parallel.

$$\boldsymbol{x}_{\mathrm{k}+1}^i = \boldsymbol{x}_{\mathrm{k}}^i + \tau(z_{\mathrm{k}+1}^i - g_{\mathrm{B,k}+1}) \tag{31}$$

From the above iteration steps, it can be seen that each sub-problem can be solved in parallel, which greatly reduces the difficulty of problem solving caused by the increase of scenarios and ensures the convergence of the algorithm. In addition, an adaptive dual updating step τ is introduced to ensure the convergence speed. The convergence of each sub-problem is judged on its own terms. According to the principle

of ADMM, the primal residual $\boldsymbol{\varphi}_{\mathrm{k}}^{\mathrm{p}}$ and dual residual $\boldsymbol{\varphi}_{\mathrm{k}}^{\mathrm{d}}$ are used as convergence indicators.

$$\left\|\boldsymbol{\varphi}_{\mathrm{k}+1}^{\mathrm{p}}\right\|_2=\sqrt{\frac{1}{I}\sum_{i\in I}\left\|\mathbf{z}_{\mathrm{k}+1}^{i}-g_{B,k+1}^{i}\right\|_2^2} \tag{32}$$

$$\left\|\boldsymbol{\varphi}_{\mathrm{k}+1}^{\mathrm{d}}\right\|_2=\tau\sqrt{\left(g_{\mathrm{k}+1}-g_{\mathrm{k}}\right)^{\mathrm{T}}\left(g_{\mathrm{k}+1}-g_{\mathrm{k}}\right)} \tag{33}$$

The update rule of τ is as follows:

$$\tau_{\mathrm{k}+1}=\begin{cases}r_1\tau_{\mathrm{k}} & \text{if } \left\|\boldsymbol{\varphi}_{\mathrm{k}}^{\mathrm{p}}\right\|_2>r_2\left\|\boldsymbol{\varphi}_{\mathrm{k}}^{\mathrm{d}}\right\|_2\\ \tau_{\mathrm{k}}/r_1 & \text{if } \left\|\boldsymbol{\varphi}_{\mathrm{k}}^{\mathrm{d}}\right\|_2>r_2\left\|\boldsymbol{\varphi}_{\mathrm{k}}^{\mathrm{p}}\right\|_2\\ \tau_{\mathrm{k}} & \text{otherwise}\end{cases} \tag{34}$$

where $r_1>1$ and $r_2>1$. The convergence condition of the algorithm is:

$$\left\|\boldsymbol{\varphi}_{\mathrm{k}+1}^{\mathrm{p}}\right\|_2\le N_{\mathrm{p}},\left\|\boldsymbol{\varphi}_{\mathrm{k}+1}^{\mathrm{p}}\right\|_2\le N_{\mathrm{d}} \tag{35}$$

where N_{p} and N_{d} are a certain threshold determined by absolute and relative convergence rates.

C. Theoretical Analysis of the GSFTO Algorithm

Based on the basic structure of FTO [34], the Fibonacci tree is constructed by two iterative rules. Let $|R|=F_i$. $\boldsymbol{x}_{\mathrm{m}}$, $\boldsymbol{x}_{\mathrm{n}}$ and $\boldsymbol{x}_{\mathrm{s}}$ satisfies the linear relationship as:

$$\boldsymbol{x}_{\mathrm{s}}=\frac{F_i}{F_{i+1}}\left(\boldsymbol{x}_{\mathrm{n}}-\boldsymbol{x}_{\mathrm{m}}\right)+\boldsymbol{x}_{\mathrm{m}} \tag{36}$$

Rule 1: Let $\{\boldsymbol{x}\}_{\mathrm{m}}=R$ and $\{\boldsymbol{x}_{\mathrm{n}}\}=\left\{\boldsymbol{x}\middle|\boldsymbol{x}\in\prod_{i=1}^{W}[x_{\mathrm{lb}}^{i},x_{\mathrm{ub}}^{i}]\right\}$, respectively. x_{d} denotes the component of vector $x=[x_1,x_2,\ldots,x_{\mathrm{d}},\ldots,x_{\mathrm{n}}]^{\mathrm{T}}$, which satisfies a uniform distribution, and the probability distributions can be expressed as $P(X)=U(x_{\mathrm{lb}},x_{\mathrm{ub}})$. Split point set $\{\boldsymbol{x}\}_{\mathrm{s}}$ can be obtained by (36).

Rule 2: Let $\boldsymbol{x}_{\mathrm{m}}=\boldsymbol{x}_{\mathrm{fitbest}}\in R$ is the optimal solution of R, and $\{\boldsymbol{x}_{\mathrm{m}}\}=\{\boldsymbol{x}|x\in R\wedge\boldsymbol{x}\neq\boldsymbol{x}_{\mathrm{m}}$ Split point set $\{\boldsymbol{x}\}_{\mathrm{s}}$ can be obtained by (36).

FTO is a meta-heuristic optimal algorithm based on the Fibonacci method, but the convergence ability of FTO decreases near the optimal solution. Reference [35] introduces the golden section method into the control strategy of the ultrasonic motor to improve the efficiency of the solution. This paper adopts this approach and introduces the golden section method into the FTO algorithm. So, we propose the GSFTO method to improve global optimal ability and convergence, meanwhile the solution space is updated by the optimality of the golden section method in each iterative process. The GSFTO algorithm is formulated in Algorithm 1.

The GSFTO algorithm is an intelligent optimization algorithm based on the Fibonacci method. The algorithm solves the optimal solution of the problem by alternating the iteration of global exploration and local optimization. At the same time, it makes full use of computer memory to record the optimization process. The GSFTO algorithm not only guarantees global optimization capability, but also has high local optimization capability.

It can be seen that the optimal solution is obtained by both global and local optimization, which can ensure that the algorithm can provide the local optimal solution. The Fibonacci tree growth process is based on the best of the previous generations. The search formation of the element is also a process of competition elimination. The global point is randomly generated within the entire solution space, the lower peaks will be discarded during the optimization process, thus the integrity of the algorithm information is reduced.

In the growth process of the Fibonacci tree, the golden space segmentation compression is performed on the solution space, so that the search elements have different optimization ranges at different levels. In addition, the optimality of GS can be used to determine whether the current iteration needs the most advantageous information from the last iteration. The information can be utilized if the advantage of the last iteration is within the solution space of the current iteration, otherwise, the information of the last iteration will be discarded. Therefore, the GSFTO algorithm can ensure the global optimization ability while improving its local optimization abilities, and the convergence of the algorithm is improved.

Algorithm 1 GSFTO Algorithm

Initialization: iteration index $N=1$, $|R|=F_i$, $N_{\max}$;
1: **for** N = 1: $N_{\max}$ **do**
2: Obtain $\{\boldsymbol{x}_{\mathrm{n}}\}$ and $\{\boldsymbol{x}_{s1}\}$ using the *Rule 1* with $F_i/F_{i+1}=0.618$;
3: Obtain $\{\boldsymbol{x}_{s2}\}$ using the *Rule 2* with $F_i/F_{i+1}=0.618$;
4: Merge R, $\{\boldsymbol{x}_{\mathrm{n}}\}$, $\{\boldsymbol{x}_{s1}\}$ and $\{\boldsymbol{x}_{s2}\}$;
5: **if** $F_{i+1}<N_{\max}$ **then**
6: F_{i+1} advantage points are retained;
7: $|R|=F_{i+1}$;
8: **else**
9: $N_{\max}$ advantage points are retained;
10: $|R|=N_{\max}$
11: **end if**
12: **end for**

D. Hierarchical Optimization Algorithm

The steps of the hierarchical optimization algorithm proposed in this paper are as follows:

Step 1: E_{w} and E_{pv} are initialized using the GSFTO algorithm in the upper level;

Step 2: The initial capacity obtained in Step 1 is introduced into the lower level model. Combined with the normalized time sequence power of wind and solar energy obtained from the TSS method, the respective theoretical time sequence power is obtained. The distributed manner is adopted to solve the consensus problem, and the minimum investment cost of the system under the optimal energy storage capacity is obtained;

Step 3: The initial E_{w} and E_{pv} and the optimal ESS power are introduced to the upper level model. The GSFTO method is adopted to optimize $E_{\mathrm{w}}/E_{\mathrm{pv}}$;

Step 4: The optimized $E_{\mathrm{w}}/E_{\mathrm{pv}}$ in Step 3 are returned again to the lower level model, and the calculation is continued. Thus, the updated investment cost of the system is obtained;

Step 5: Repeat Step 2–Step 4 for the iterative calculation until the termination condition $k<N_{\max}$ is met;

Step 6: When the calculation is completed, the optimal $E_{\mathrm{w}}/E_{\mathrm{pv}}$ and ESS capacity can be obtained.

The flow chart of the hierarchical optimization algorithm is shown in Fig. 1.

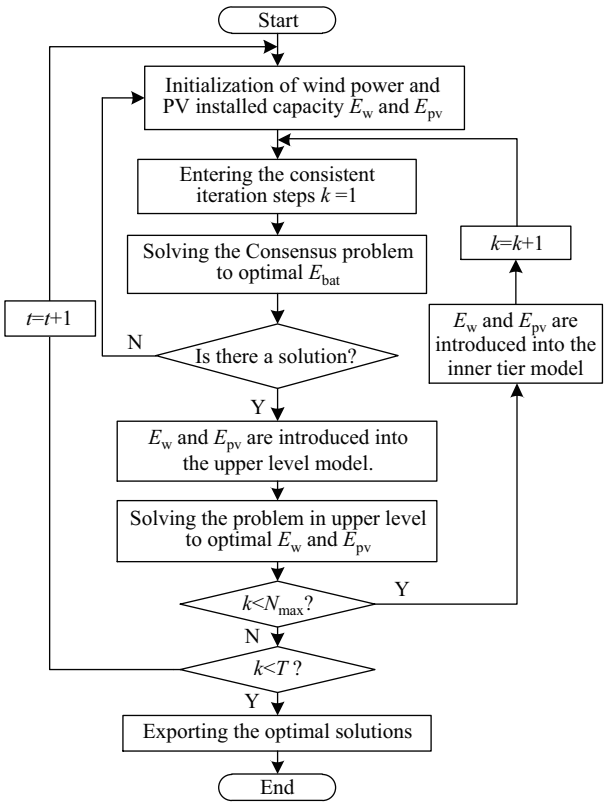

Fig. 1. Flow chart of hierarchical optimization algorithm.

V. Case Studies

A number of cases using data processed using TSS are provided to illustrate how the proposed model and method are helpful to obtain RE generation and ESS capacity.

A. System and Data

A high penetration RE system in northern China is tested in this paper; the schematic diagram of the system is shown in Fig. 2, in which the total wind and PV capacity is 620 MW. It can be seen that the power supply of this system is only wind power and PV power, so this is strictly a 100% RE penetration system. All plants converge on two 220 kV transformer substations. In order to ensure that the RE sequence can reflect

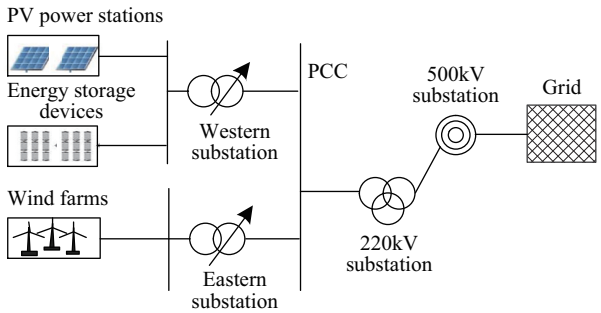

Fig. 2. Schematic diagram of multi energy system.

its volatility and randomness, this paper uses the TSS method to generate RE sequence in the lower level. The wind and PV power time sequences of four typical days in each season and the whole year are depicted in Fig. 3. The utilization hours of wind and PV power are 1,975 hours and 1,529 hours respectively. One-year of data for the TSS method is used in the test case, the planning horizon in this paper is a whole year, Δt is set to 1 h, the sub planning horizon is 7 days, so $T = 24 \times 7 = 168$, $J = 52$. Table I shows the parameters.

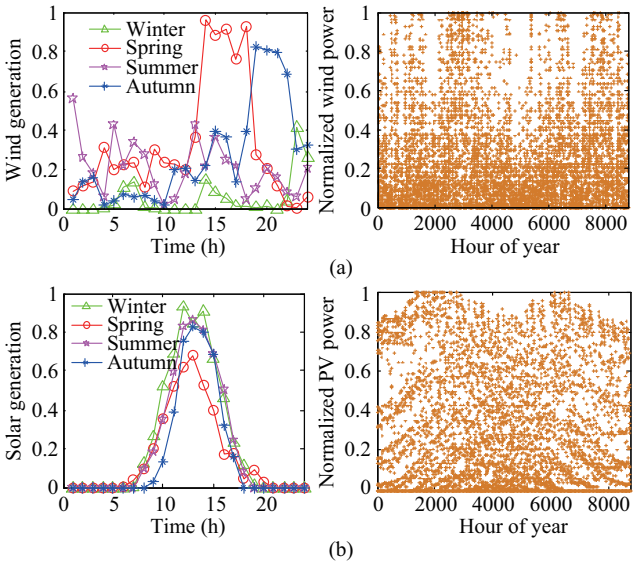

Fig. 3. Renewable power time sequences. (a) Typical days and hourly values of annual wind power. (b) Typical days and hourly values of annual PV power.

TABLE I
Simulation Parameters

c^1_{inv} (¥/Wh)	c^2_{inv} (¥/Wh)	c_w (¥/Wh)	c_{pv} (¥/Wh)	ϖ^s_{min}	ϖ^s_{max}	η_{RE} (%)
0.218	0.0068	0.377	0.826	0.2	0.95	5

In this paper, the network constraints are not included in the model. It can be seen that all the power sources in this test system are concentrated in a very close space and can be equivalent to a large power source. According to the practical operational experience, the simplification we adopted has little effect on the results of system planning. So, the network constraints are neglected in this special test system.

B. Determination of Boundary Parameters

In practice, the transmission line capacity is designed according to total generation, let P_{line} denote the capacity proportion of the transmission line to the total generation. Table II shows the ESS capacity and the curtailment rate of RE under different P_{line}. We can see that the ESS capacity and RE curtailment rate both decrease with the increasing of P_{line}. The results show the optimal ESS capacity is relatively close and all RE curtailment rates are less than 5%. Thus, P_{line} is chosen as 40% in this section.

Let $N_{max} = 5$ in the GSFTO algorithm. The calculation results are shown in Fig. 4. E_w/E_{pv} is given as 0.5 to 2. We can see that when $E_w/E_{pv} = 1$, the curtailment rate is at a

TABLE II
INFLUENCE OF THE CAPACITY PROPORTION OF TIE-LINE TO TOTAL GENERATION ON OPERATIONS

P_{line} (%)	E_{bat} (MW·h)	η_{RE} (%)
40	137.92	4.66
45	136.74	3.28
50	135.81	2.24
55	133.77	1.37
60	131.56	0.84

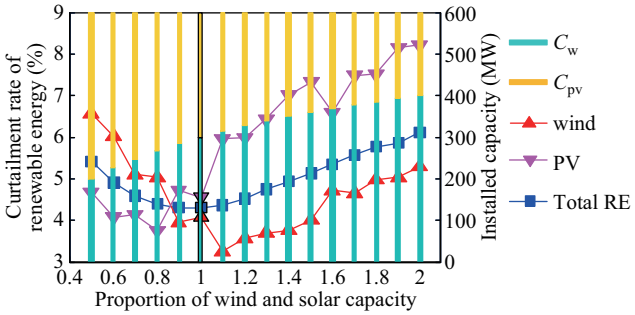

Fig. 4. Curve between the proportion of wind and PV capacity and the RE curtailment rate.

minimum of 4.47%. So, it is chosen as both the initial capacity of wind and PV power and is set to 310 MW.

C. Comparison of Results with Different Methods

Let η_{w} and η_{pv} denote the curtailment rates of wind and PV power respectively. When the $E_{\text{w}}/E_{\text{pv}} = 1$ and $P_{\text{line}} =$ 248 MW (620 $\times$ 40%). The calculation results are shown in Table III, the capacity of the ESS battery is 107.05 MW and the RE curtailment rate is down to 4.37%, as well as the curtailment rates of wind and PV power are 4.04% and 4.70%, respectively.

TABLE III
INDEXES OF RENEWABLE ENERGY ACCOMMODATIO

The total cost/M¥	E_{bat} (MW·h)	η_{RE} (%)	η_{w} (%)	η_{pv} (%)
414.37	107.05	4.37	4.04	4.70

Except for the proposed method, others methods are used to optimize the capacity of wind and solar power in this system. Method 2 is to replace the upper level search algorithm of method 1 with the PSO algorithm. The parameters in the PSO algorithm are set as follows: number of particles $m = 3$, particle inertia coefficient $w = 0.4$, learning factor $c_1 = c_2 = 2$, the maximum/minimum inertia weights $w_{\max} = 0.9/w_{\min} = 0.4$, the maximum convergence speed $V_{\max} = 0.03$, and the sampling period $T_{\text{PSO}} = 0.015$ [29]; Method 3 replaces the generating RE sequence method in the lower level of method 1 with the typical day method. The wind and PV output of a typical day in each season are selected to simulate the annual output. The typical daily curve we selected here is shown in Fig. 4. Table IV shows the optimization results of different methods.

Method 1 is the hierarchical optimization algorithm proposed in this paper. Comparing methods 1 and 2, the upper level model using the GSFTO algorithm can effectively improve the calculation accuracy, the total investment cost is reduced by 1.23%, and the calculation time is reduced by

TABLE IV
OPTIMAL SOLUTIONS OF DIFFERENT METHODS

method	Upper level algorithm	Lower level algorithm	The ESS cost(M¥)	E_{w} (MW)	E_{pv} (MW)	Calculation time (min)
1	GSFTO	ADMM &TSS	414.37	306	294	5.4
2	PSO	ADMM &TSS	419.46	313	287	7.3
3	GSFTO	ADMM &typical day	426.14	345	255	17.2
4	GSFTO	TSS	416.57	308	292	8.2
5	ADMM&TSS		418.33	312	288	10.6

35.19%. The lower level model of Method 3 uses a typical day operational mode. The four typical days of RE sequences in Fig. 3 are used in Method 3. This mode considers the reception of wind power and PV power in the most severe cases. Compared with method 1, the total investment cost increases by 2.84% and the calculation time of the method 3 model is raised by 218.52%. This result proves that the TSS method can make the planning result more reliable. In order to validate the effectiveness of the consensus problem and the distributed optimization method proposed in this paper, the results of Method 1 and Method 4 are compared. The lower level of method 4 adopts the centralized control optimization, which does not need the ADMM algorithm to solve it. The results show that the difference of the ESS cost is 0.53%, which can be considered to be very close. Compared with the centralized control optimization, the distributed control needs continuous interactive iteration because of the lack of global information, which requires a long time to obtain. However, it can effectively reduce the computational difficulty of the parallel solution. The results show that the proposed distributed method is still 34.1% more efficient than the centralized method.

Method 5 is the single-level algorithm based on ADMM & TSS, which simultaneously calculates the RE generation capacity and storage capacity. The calculation results are similar to method 2. Compared with method 1, the battery capacity obtained is 110.96 (MW·h), so total investment cost increases by 0.96%, and the calculation time is raised two times. Method 5 is limited in the application of larger-scale power systems, and the proposed algorithm has the better accuracy and efficiency.

Figure 5 shows the total RE generation and curtailment of RE under different hierarchical algorithms. Compared with the other two methods, the curtailment of RE is reduced under the proposed method 1 during all planning horizons, meanwhile the total RE generation is increased, proving the effectiveness of the proposed method in improving the RE accommodation.

D. Comparison of Results with Different RE Sequences

The results of [36] shows that if the input samples of the RE sequences have the same annual utilization hours, probability distribution characteristics and fluctuation characteristics, the planning results will be very close, and the expected values of the results within 60 times can be convergent. In this case, we use the TSS method to generate 60 sets of wind and solar energy sequences, and calculate the planning results of these samples. The results show that the optimal total cost is between

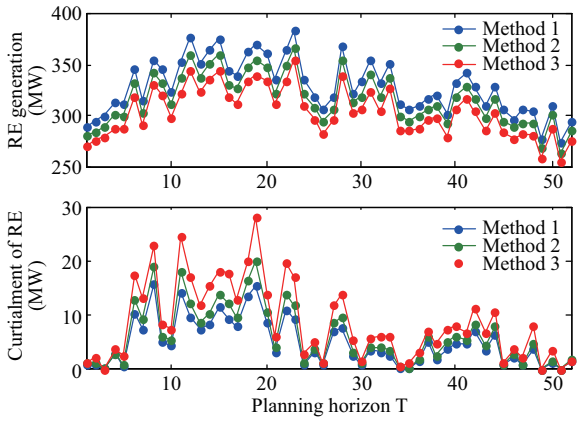

Fig. 5. Total RE generation and curtailment of RE under different algorithms.

412.86 and 417.74 M¥. Fig. 6(a) shows the convergence of expectation of the total cost. The results show that the optimal total cost converges to 414.37 M¥ with the increase of simulation times. Fig. 6(b) is the optimal wind and solar power capacity proportions of 60 samples. The results showed that the proportions of 100 stochastic sequences ranged from 1.03 to 1.05, and the mean of all results was 1.04.

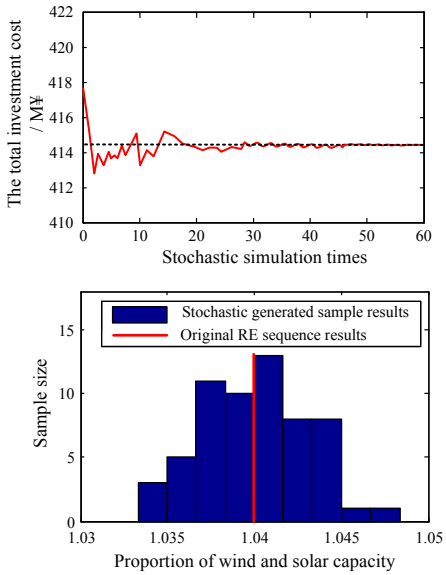

Fig. 6. Results of 60 RE sequence samples. (a) Convergence curve for expectation of the total cost. (b) The optimal wind and solar power capacity proportions.

In addition, a typical scenario of an RE station in China is taken to show the universal applicability of the proposed method, the utilization hours of wind and PV power are 2,027 hours and 1,326 hours respectively in this scenario. The results are shown in Table V. Compared with method 4, we can see that the proposed method still maintains better accuracy and efficiency of optimization, the total investment cost and the calculation time are reduced by 1.14% and 45.63% respectively, and the RE curtailment rate is down to 1.06%.

TABLE V
OPTIMAL SOLUTIONS UNDER DIFFERENT SCENARIOS

Method	The ESS cost (M¥)	E_{bat} (MW·h)	η_{RE} (%)	E_w (MW)	E_{pv} (MW)	Calculation time (min)
1	412.06	102.50	1.06	364	236	5.6
4	416.74	111.72	1.09	381	219	10.3

VI. CONCLUSION

We consider the problem of synchronously optimizing the capacity of RE generation and ESS when considering the power constraints of the tie-line, so that the research object is not limited to an isolated power grid or distributed power grid. To avoid the high-dimensional complexity caused by a long-process annual time sequence, a hierarchical method is introduced to solve the MILP model. The original lower level programming problem is redefined as a consensus problem and solved by using a parallel distributed framework, and the GSFTO algorithm is adopted to solve the problem in the upper level. The results show that the proposed method can improve the computational accuracy, and the hierarchical distributed control strategy is more effective than the single-level control when dealing with multi-objective and high-dimensional systems. TSS technology is used to describe the characteristics of RE power, as well as generating multiple sets of RE output sequences for capacity planning to increase the reliability of the planning results, and the obtained results are highly similar, which proves that the characteristics of RE resources are fully considered in this paper. In addition, the reasonable choice of boundary parameters has a noticeable impact on the calculation results. Some guidance is given for the optimal capacity of ESS and renewable generation under low RE curtailment, which potentially allows for better results with RE utilization.

REFERENCES

[1] F. Birol, "World energy outlook," International Energy Agency, Paris, France, pp. 23–29, 2014.
[2] W. W. Kim, J. S. Shin, and J. O. Kim, "Operation strategy of multi-energy storage system for ancillary services," *IEEE Transactions on Power Systems*, vol. 32, no. 6, pp. 4409–4417, Nov. 2017.
[3] Y. S. Sun, Z. X. Zhao, M. Yang, D. Q. Jia, W. Pei, and B. Xu, "Overview of energy storage in renewable energy power fluctuation mitigation," *CSEE Journal of Power and Energy Systems*, vol. 6, no. 1, pp. 160–173, Mar. 2020.
[4] Z. X. Lu, H. B. Li, and Y. Qiao, "Flexibility evaluation and supply/demand balance principle of power system with high-penetration renewable electricity," *Proceedings of the CSEE*, vol. 37, no. 1, pp. 9–19, Jan. 2017.
[5] A. V. Savkin, M. Khalid, and V. G. Agelidis, "A constrained monotonic charging/discharging strategy for optimal capacity of battery energy storage supporting wind farms," *IEEE Transactions on Sustainable Energy*, vol. 7, no. 3, pp. 1224–1231, Jul. 2016.
[6] S. Dutta and R. Sharma, "Optimal storage sizing for integrating wind and load forecast uncertainties," in *2012 IEEE PES Innovative Smart Grid Technologies* (*ISGT*), 2012, pp. 1–7.
[7] M. E. Khodayar, M. Shahidehpour, and L. Wu, "Enhancing the dispatch ability of variable wind generation by coordination with pumped-storage hydro units in stochastic power systems," *IEEE Transactions on Power Systems*, vol. 28, no. 3, pp. 2808–2818, Aug. 2013.
[8] L. Shi, Y. Luo, G. Y. Tu, and N. Shi, "Energy storage sizing method considering dispatch ability of wind farm," *Transactions of China Electrotechnical Society*, vol. 28, no. 5, pp. 120–127, 134, May. 2013.
[9] O. Mégel, J. L. Mathieu, and G. Andersson, "Scheduling distributed energy storage units to provide multiple services under forecast error," *International Journal of Electrical Power & Energy Systems*, vol. 72, pp. 48–57, Nov. 2015.

[10] S. Lakshminarayana, Y. J. Xu, H. V. Poor, and T. Q. S. Quek, "Cooperation of storage operation in a power network with renewable generation," *IEEE Transactions on Smart Grid*, vol. 7, no. 4, pp. 2108–2122, Jul. 2016.
[11] P. Yang and A. Nehorai, "Joint optimization of hybrid energy storage and generation capacity with renewable energy," *IEEE Transactions on Smart Grid*, vol. 5, no. 4, pp. 1566–1574, Jul. 2014.
[12] H. Alharbi and K. Bhattacharya, "Stochastic optimal planning of battery energy storage systems for isolated microgrids," *IEEE Transactions on Sustainable Energy*, vol. 9, no. 1, pp. 211–227. Jan. 2018.
[13] S. S. Thale, R. G. Wandhare, and V. Agarwal, "A novel reconfigurable microgrid architecture with renewable energy sources and storage," *IEEE Transactions on Industry Applications*, vol. 51, no. 2, pp. 1805–1816, Mar. 2015.
[14] A. Kargarian, G. Hug, and J. Mohammadi, "A multi-time scale co-optimization method for sizing of energy storage and fast-ramping generation," *IEEE Transactions on Sustainable Energy*, vol. 7, no. 4, pp. 1351–1361, Oct. 2016.
[15] J. J. Dong, F. Gao, X. H. Guan, Q. Z. Zhai, and J, Wu, "Storage-reserve sizing with qualified reliability for connected high renewable penetration micro-grid," *IEEE Transactions on Sustainable Energy*, vol. 7, no. 2, pp. 732–743, Apr. 2016.
[16] D. Bhowmik and A. K. Sinha, "Cost-based allocation model for hybrid power system considering solar, wind and thermal generations separately," *IET Generation, Transmission & Distribution*, vol. 11, no. 18, pp. 4576–4587, Dec. 2017.
[17] E. Nasrolahpour, J. Kazempour, H. Zareipour, and W. D. Rosehart, "Impacts of ramping inflexibility of conventional generators on strategic operation of energy storage facilities," *IEEE Transactions on Smart Grid*, vol. 9, no. 2, pp. 1334–1344, Mar. 2018.
[18] C. J. López-Salgado, O. Añó, and D. M. Ojeda-Esteybar, "Stochastic unit commitment and optimal allocation of reserves: a hybrid decomposition approach," *IEEE Transactions on Power Systems*, vol. 33, no. 5, pp. 5542–5552, Sep. 2018.
[19] M. Alsayed, M. Cacciato, G. Scarcella, and G. Scelba, "Multicriteria optimal sizing of photovoltaic-wind turbine grid connected systems," *IEEE Transactions on Energy Conversion*, vol. 28, no. 2, pp. 370–379, Jun. 2013.
[20] S. F. Santos, D. Z. Fitiwi, M. Shafie-Khah, A. W. Bizuayehu, C. M. P. Cabrita, and J. P. S. Catalão, "New multistage and stochastic mathematical model for maximizing RES hosting capacity-Part I: problem formulation," *IEEE Transactions on Sustainable Energy*, vol. 8, no. 1, pp. 304–319, Jan. 2017.
[21] A. Arabali, M. Ghofrani, M. Etezadi-Amoli, and M. S. Fadali, "Stochastic performance assessment and sizing for a hybrid power system of solar/wind/energy storage," *IEEE Transactions on Sustainable Energy*, vol. 5, no. 2, pp. 363–371, Apr. 2014.
[22] E. F. M. Abreu, P. Canhoto, V. Prior, and R. Melicio, "Solar resource assessment through long-term statistical analysis and typical data generation with different time resolutions using GHI measurements," *Renewable Energy*, vol. 127, pp. 398–411, Nov. 2018.
[23] T. Qiu, B. L. Xu, Y. S. Wang, Y. Dvorkin, and D. S. Kirschen, "Stochastic multistage coplanning of transmission expansion and energy storage," *IEEE Transactions on Power Systems*, vol. 32, no. 1, pp. 643–651, Jan. 2017.
[24] M. Trifkovic, M. Sheikhzadeh, K. Nigim, and P. Daoutidis, "Modeling and control of a renewable hybrid energy system with hydrogen storage," *IEEE Transactions on Control Systems Technology*, vol. 22, no. 1, pp. 169–179, Jan. 2014.
[25] Y. Cao, Y. H. Huang, Y. Yuan, M. Wang, P. Li, and S. Q. Guo, "Stratified optimization algorithm for optimal proportion of wind and solar capacity based on time sequence simulation," *Proceedings of the CSEE*, vol. 35, no. 5, pp. 1072–1078, Mar. 2015.
[26] S. Baros and M. D. Ilić. "A consensus approach to real-time distributed control of energy storage systems in wind farms," *IEEE Transactions on Smart Grid*, vol. 10, no. 1, pp. 613–625, Jan. 2019.
[27] Q. Y. Sun, R. K. Han, H. G. Zhang, J. G. Zhou, and J. M. Guerrero, "A multiagent-based consensus algorithm for distributed coordinated control of distributed generators in the energy Internet," *IEEE Transactions on Smart Grid*, vol. 6, no. 6, pp. 3006–3019, Nov. 2015.
[28] Y. Dong, D. J. Lv, X. Wang, Y. M. Wang, P. Li, and X. L. Shi, "A global randomness-based probability convergence analysis of Fibonacci tree optimization algorithm," *Control and Decision*, vol. 33, no. 3, pp. 439–446, Mar. 2018.
[29] F. Alismail, P. Xiong, and C. Singh, "Optimal wind farm allocation in multi-area power systems using distributional robust optimization approach," *IEEE Transactions on Power Systems*, vol. 33, no. 1, pp. 536–544, Jan. 2018.
[30] X. X. Zhu and Z. H. Han, "Research on LS-SVM wind speed prediction method based on PSO," *Proceedings of the CSEE*, vol. 36, no. 23, pp. 6337–6342, Dec. 2016.
[31] X. D. Ke, N. Lu, and C. L. Jin, "Control and size energy storage systems for managing energy imbalance of variable generation resources," *IEEE Transactions on Sustainable Energy*, vol. 6, no. 1, pp. 70–78, Jan. 2015.
[32] P. D. Brown, J. A. P. Lopes, and M. A. Matos, "Optimization of pumped storage capacity in an isolated power system with large renewable penetration," *IEEE Transactions on Power Systems*, vol. 23, no. 2, pp. 523–531, May. 2008.
[33] Y. M. Wang, L. Wu, and S. X. Wang. "A fully-decentralized consensus-based ADMM approach for DC-OPF with demand response," *IEEE Transactions on Smart Grid*, vol. 8, no. 6, pp. 2637–2647, Nov. 2017.
[34] S. H. Zhang, X. L. Shi, P. Li, Y. Dong, and S. C. Li, "Golden section Fibonacci tree optimization algorithm for multimodal function optimization," *Acta Electronica Sinica*, vol. 45, no. 4, pp. 791–798, Apr. 2017.
[35] J. Z. Shi and D. M. You, "Golden section adaptive speed control of ultrasonic motors," *Transactions of China Electrotechnical Society*, vol. 28, no. 6, pp. 59–65, Jun. 2013.
[36] M. Ding, M. J. Chu, R. Bi, and W. H. Shi, "Wind power accommodation capability evaluation based on sequential Monte Carlo probabilistic production simulation and its application," *Electric Power Automation Equipment*, vol. 36, no. 9, pp. 67–73, Sep. 2016.

Zhaodi Shi received the B.E. and M.E. degrees both in Electrical Engineering, from Xi'an University of Technology, Xi'an, China, in 2014 and 2017, respectively. She is currently working toward the Ph.D. degree in Electrical Engineering of China Electric Power Research Institute, Beijing, China.

Her research interests include capacity planning and dispatching operation technology renewable energy generation.

Weisheng Wang received the Ph.D. degree in Electrical Engineering from Xi'an Jiaotong University, Xi'an, China, in 1996. Presently, he is the director of Department of renewable energy, China Electric Power Research Institute (CEPRI) and his research interests include wind power generation, power system simulation and analysis, renewable energy integration and control aspects of renewable energy.

Prof. Wang was awarded Science and Technology Progress Prize of CEPRI and SGCC in 2006 and 2007 respectively. He has published three books and over twenty technical papers.

Yuehui Huang received the B.S. and M.S. degree from Xi'an Jiaotong University in 2002 and 2005 respectively, both in Electrical Engineering. In 2008, She received the Ph.D. degree in Electronic Information Engineering from The Hong Kong Polytechnic University in the department of Electronic and Information Engineering, Hong Kong, China, in 2008.

Currently, she is a Professorate Senior Engineer in China Electric Power Research Institute (CEPRI), Beijing. Her research interests include renewable generation integration and its dispatch and operation technology.

Pai Li received the B.S. degree in Automatic Control from Xi'an Jiaotong University, Xi'an, China, in 2009, and the Ph.D. degree in Systems Engineering from the same university, in 2015. He is currently a Senior Engineer in China Electric Power Research Institute.

His interests include power system production simulation and scheduling with renewable energy.

Ling Dong received the M.S. degree in Power System and Automation from North China Electric Power University, Beijing, China. Currently, she is serving as deputy director of Qinghai Electric Power Dispatching and Control Center and is currently studying for a Ph.D. degree in Tsinghua University. Her research interests include power grid dispatching and operation.